2016
International Symposium on Power Electronics,
Electrical Drives, Automation and Motion

Influence of Current Transducer Transfer Properties on Stator Insulation Condition Monitoring of Inverter-fed Drives

C. Zoeller*), M.A. Vogelsberger**), Walter Fahrner*), Th.M. Wolbank*)

*) Institute of Energy Systems and Electrical Drives
Vienna University of Technology
Vienna, Austria

**) Internal Supply Chain (ISC/M); Drives, Vienna
Bombardier Transportation Austria GmbH
Vienna, Austria

Abstract—**Insulation condition monitoring is important in case of inverter-fed machines due to the high strains on the machine and especially on its winding insulation system. In particular in traction applications the usage of new emerging semiconductor technologies, which enable higher inverter switching frequencies and rapid voltage rises, transient overvoltages at the machine occur. The insulation system suffers due to these overvoltages and a reduced lifetime and increased risk of unexpected outage of the drive are the consequences. A strategy to monitor the insulation health state during the operation of the drive based on transient current signal evaluation to detect incipient insulation degradation enables the possibility to define further maintenance tasks. Using only the measuring equipment available in the inverter, space and costs of the monitoring system are optimized. Experimental results of this concept, tested at a 1.4MW induction machine for railway application are presented. Additionally, the variance in the transfer function of different current transducer's of the same type and its influence on the proposed method is analyzed.**

Keywords—AC machines; current measurement; fault diagnosis; insulation; electric breakdown;

I. INTRODUCTION

In this paper, a method for monitoring the insulation state in a drive system based on the analysis of transient oscillations in the current signal at inverter switching is presented. By evaluation of the occurring frequency components at the transient current response after inverter switching transition, a change in the insulation health state can be detected. First investigations based on the method are presented in [1]-[2] and are enhanced with the investigations in this paper.

In traction applications, the fast switching transients of modern voltage source inverters (VSI) lead to transient overvoltage at the machine as was analyzed in several studies [3]-[4]. With new emerging wide-band gap semiconductor technologies and as a consequence thereof increasing switching speed of the inverter (high dv/dt rates), additional stress on the motor winding insulation exists and may lead to a deterioration of the insulation strength and a reduced lifetime with unexpected outage of the drive. Further stresses can be stated, e.g. thermal, mechanical or environmental stress, that all affect the electrical strength of the insulation system. These main causes responsible for insulation deterioration have been analyzed in [5]-[6]. A statement about the probability of an outage of a machine due to a stator fault can only be specified in connection with the electrical power and voltage of the machine. In [7] the appearance of a stator related fault is about 35-40% for medium voltage induction motors. For high voltage machines about 70% of these stator faults are based on a failure of the insulation system [8]-[9].
Most monitoring methods able to estimate the health state of an insulation system like dissipation factor tan(δ) tip-up, partial discharge PD, polarization index PI) are currently based on either offline measurements or extensive measurement equipment and are usually linked to experienced examiners. Compared to other methods the approach investigated in this paper is able to detect imminent insulation degradation and does not need any additional test or measurement equipment.

With the strategy to estimate the insulation state of the machine with the built-in current transducers of the inverter, no additional sensor hardware is required and costs are kept as low as possible. Since the drive does not need to be disassembled, the test procedure can be implemented during or at least at the beginning of the operation of the drive, to test the insulation state in shorter intervals than in case of conventional maintenance, which are complex and need the drive to be set out of service. This enables to detect incipient insulation degradation and enables scheduled maintenance on demand.

Insulation degradation is usually a slowly proceeding process, sometimes even over decades and has not been analyzed over such a long time for a traction drive systems. Therefore, it is a common practice to use accelerated aging to describe the process and effects of insulation degradation. In [10] and [11] tests with accelerated insulation aging conducted with thermal exposure cycles on stator coils show that the parameter which is mainly influenced by the changes of the material is the insulation capacitance. The capacitance values of the specimens have changed over time and with the number of aging cycles. These effects can be observed at high voltage tests with several time of the nominal voltage [10] as well as at low voltage tests over a wide frequency range [12]. The capacitance is in all cases usually considered as the dominant parameter for insulation health state evaluation. The winding capacitance can be seen as a parasitic component in a drive system, which does not contribute anything to the energy

978-1-5090-2067-6/16/$31.00 ©2016 IEEE

conversion from electrical to mechanical power. However, a change in the insulation system which is accompanied by a change in the insulation capacitance value also affect the transient high frequency behavior of the current response of the machine. A detailed description of the evaluation of the insulation state based on these facts is given in the next chapter.

II. Insulation State by Transient Current Response Evaluation

The insulation health state monitoring method is based on analysis of the transient current reaction to a voltage step excitation of all phases. The excitation is conducted with the inverter connected to the machine to enable the variable speed drive independent from the connected grid frequency. The inverter consists of three half-bridges, each built-on two power semiconductor switches which are controlled complementarily. For the investigations in this work, two semiconductor types, IGBT as well as SiC technology are used with dv/dt-rates up to 3-4kV/µs in case of IGBT and 20kV/µs for SiC power semiconductor. With the inverter, every machine phase is excited separately. By executing a simple switching transition, starting with all three half-bridge outputs at low side of DC-link and turning on the high side transistor of the corresponding phase, a voltage change with high gradient is applied to the machine phase. As aforementioned in the introduction, the usage of voltage source inverter leads to overvoltages and high frequency resonances at the machine terminal and within the winding system. These overvoltage oscillations are decaying in magnitude showing typical frequency components in the range of tens kHz to tens MHz, as depicted in Fig. 1 – upper figure. Different facts influence the shape and the duration of the voltage oscillation, for instance the higher machine's impedance compared to the impedance of the cabling. This phenomenon can be described by traveling wave theory [13]. The transient phenomenon is also visible in the phase current response at the instant of the switching transition and is also influenced by reflection phenomena of the fast propagated wave applied to the machine phase. Due to the fact that the frequency components of the transient are partially outside the specified frequency range of industrially applied current sensors, two measurements are compared in the lower subfigures of Fig. 1. The left subfigure shows the current response recorded with a Rogowski coil with bandwidth specification of f_{3dB}~16MHz. The right subfigure shows the current trace recorded with the built-in current transducers of the inverter (Hall-effect based closed-loop transducers) with a bandwidth specification of f_{3dB}~150kHz. As the frequency range of interest is outside the specification of the second sensor the signal accuracy is clearly reduced, however the characteristics of the transient process is well captured by the second sensor and is still reproducible. Target and key requirements of the proposed online insulation monitoring technique is the usage of the already existing sensors only. Thus in the following part of the paper, influences and effects on the method due to the low bandwidth specification of the Hall-effect closed loop transducers are analyzed.

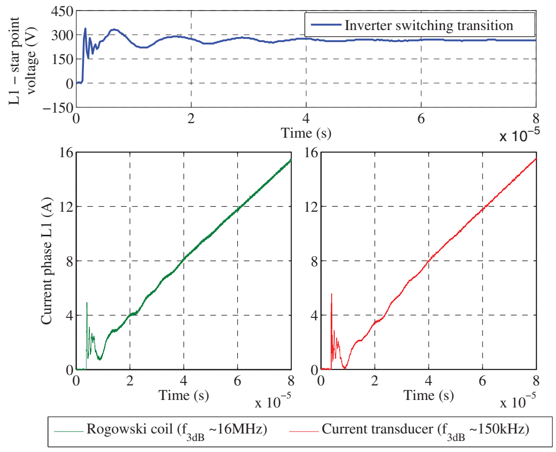

Fig. 1 Voltage phase terminal L1 to star point and current signals in phase L1.

Monitoring of insulation degradation of the machine winding has to be done over a longer period of time due to the slowly developing aging process. Usually the deterioration start with the turn-to-turn insulation and finally affecting phase-to-phase or phase-to-ground insulations. In this paper the investigations are intended to be performed during each startup of a drive and are not implemented during normal operation. However, the machine does not need to be separated from the inverter and cabling. In this work the degradation of the insulation system of the test machine (1.4MW induction machine, depicted in Fig. 2 a) is emulated with a capacitor placed parallel to parts of the winding system. Therefore, the test machine is equipped with fiber-insulation wires and additional taps accessible at terminal connection block.

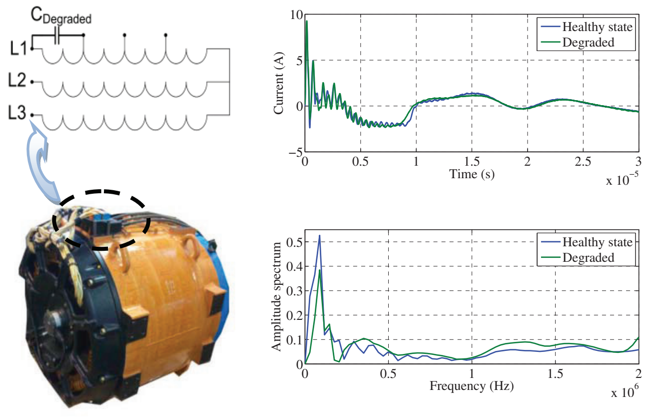

(a) (b)

Fig. 2 a) Machine and winding system b) time signals and spectra phase L1.

Different degradation scenarios can thus be analyzed by varying the position and size of the capacitor. Despite the fact that the capacitors parallel to the winding increase the total capacitance and in previous works accelerated aging tests showed a decrease of the value, the method proposed gives evidence which deviations and dimensions of capacitance variations are detectable.

For the estimation of the insulation health state simple signal processing steps are necessary to extract the information from the transient part of the current signal. In Fig. 2 (b) - upper subfigure, the time signals recorded in phase L1 of the gradient-free current traces are depicted, in order to eliminate the fundamental wave inductive component and slotting. Two machine states are shown, first the 'Healthy' state representing the machine without any variation, serving as a reference signal, and second the 'Degraded' case at which a 3nF capacitor is placed in parallel to the first coil of phase L1. A deviation in the transient current trace is still observable, even if only a small capacitor value of 3nF is added in parallel to a single coil, in comparison to the total capacitance of the phase of 21nF. The used current transducers are designed for traction applications to measure bipolar AC & DC nominal currents of up to1000 A_{rms}. Since the value of the excitation voltage is very low (compared to rated) for testing purposes, each strand is passed twice through the sensor to obtain higher current values. In the lower subfigure of Fig. 2 (b) the spectra of the transient current traces are depicted, showing a deviation over a wide frequency range up to 2MHz. The traces in these figures represent the mean values of 50 consecutive conducted measurements for each machine state to enable statistical analysis. Based on the root mean square deviation between the 'Healthy' and 'Degraded' trace for every equidistant frequency point within a defined frequency range an indicator is calculated to assess the severity of the insulation degradation. For previous investigations a frequency range from 50kHz to 1MHz is selected assuming and considering the following points:

- higher variance of frequency components <50kHz due to mean current slope calculation with low quantity of sampling points at transient part of the signal; effects due to windowing
- higher variance of frequency components >1MHz due to EMI
- low ADC sampling rate in target application
- machine type and nominal power
- sensor type

Further implementation details and descriptions of the indicator calculation process are given in [6]. Fig. 3 depicts the resulting indicators for different machine states, at which different capacitors are placed in parallel to the first coil of phase L1 to emulate a change in the winding capacitance and ongoing insulation degradation. A monotonic increase of the indicator is observable.

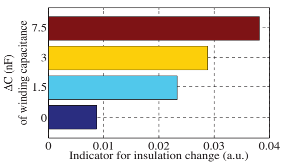

ΔC (nF)	ISI
0 (Healthy)	$8.71*10^{-3}$
1.5	$23.2*10^{-3}$
3	$28.8*10^{-3}$
7.5	$38.2*10^{-3}$

Fig. 3 Insulation state indicator at variation of winding capacitance.

In the further course of the work the frequency range was extended up to 2MHz in spite of the disadvantages described above, because certain effects that are investigated in later sections of the work are more distinct in this upper frequency area.

A. Investigation of dispersion same sensors

This chapter describes the aspects of the influences of a sensor exchange in case of an outage or exchange of the sensor hardware. Due to the implementation as a comparative method it is important that the proposed approach is immune to the influence of a change in sensor hardware. The frequency response of the sensors in the low frequency range is mainly determined by the Hall-element and the integrated circuit chip that contains the Hall-element and the signal conditioning electronics. In a higher frequency range the transfer characteristic is primarily defined by the secondary coil, acting as a current transformer delivering the compensation and output current. In this frequency range the response between different sensors indicates significant deviations, also partly within the same production batch. In Fig. 4 the difference in the magnitude and the phase frequency response of respectively two sensors of the same type and production batch are shown by analyzing the input-output transfer function at sinusoidal signals. The difference traces for both sensors of type '1' (blue traces) show higher deviations in the lower frequency below 200kHz in the magnitude and phase trace. The characteristics of the two sensors of type '2' seem to differ mainly in the higher frequency range and at the anti-resonance at 200kHz.

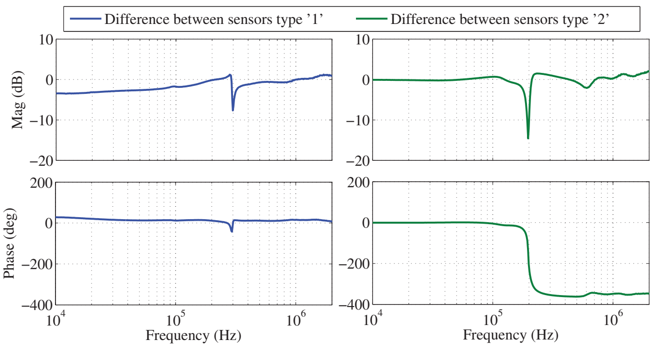

Fig. 4 Difference curve of magnitude and phase for two current transducers of type sensor 1 and two current sensors of type sensor 2.

A replacement of the sensor would have unwanted effects on the monitoring method. Thus, a compensation method is implemented to avoid deviations caused by the usage of different sensor hardware. In Fig. 5 the scenario of a sensor replacement after insulation degradation in an early stage emulated with a capacitor parallel to the first coil of phase L1 is depicted with the spectra of the resulting current signals at different machine states. The blue trace denoted 'Reference (S0)' represents the healthy machine and is used for the comparison process as the reference. The calculations for every machine state are related to this trace. The addendum 'S0' in parentheses identifies the used sensor hardware. The green curve with the donation 'Degraded ΔC=1.5nF (S0)' show the measurement of the current with the same sensor at the machine with emulated insulation degradation (capacitor of 1.5nF parallel first coil of phase L1). For comparison purposes the results 'Degraded ΔC=1.5nF (S1)' show the same machine state measured with the second sensor of the same type and producer. The larger deviations compared to the reference are clearly observable and would result in a higher indicator value and cause misinterpretation or fault alarms of the insulation state. Thus a compensation algorithm is used based on equation (1) to compensate the different characteristics of the sensors. The obtained curve is also visible in Fig. 5, denoted with 'Reference (S1) - compensated'. The variable $Y_{(S0),ad}(f_i)$ in equation (1) represents the array of the values of the new adaptive reference for each equidistant frequency point f_i ($50kHz \leq f_i \leq 2MHz$). The index deg denotes the values of the measurements of the already degraded insulation state.

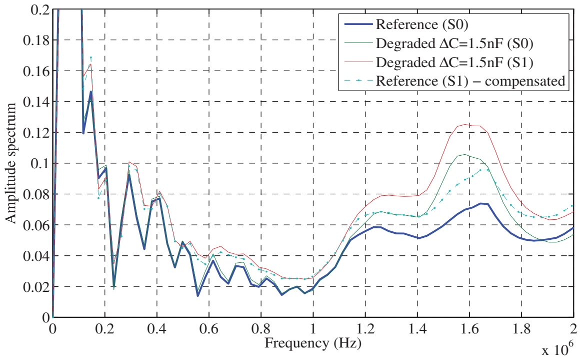

Fig. 5 Amplitude spectra recorded with different sensors and machine states and calculated compensated reference spectrum.

$$Y_{(S0),ad}(f_i) = Y_{(S0)}(f_i) - Y_{(S0),deg}(f_i) + Y_{(S1),deg}(f_i) \qquad (1)$$

The calculated indicators for the different machine states measured with both sensors, the exchange of the sensors and the applied compensation algorithm are shown in Fig. 6. Both sensors 'S0' and 'S1' respectively, measure the states with similar ISI results if the reference data is obtained with the same sensor. If a sensor is exchanged, for instance at the machine state with already degraded insulation (capacitor 1.5nF parallel to the first coil) and the measurements are continued with new sensor hardware, the indicators are higher and indicate an advanced stage of the insulation change, denoted with 'S0 (Healthy) -> S1'. Only after the compensation curve is calculated and taken as a new reference the indicators show the same magnitude and tendency as without sensor exchange (S0->S1 compensated).

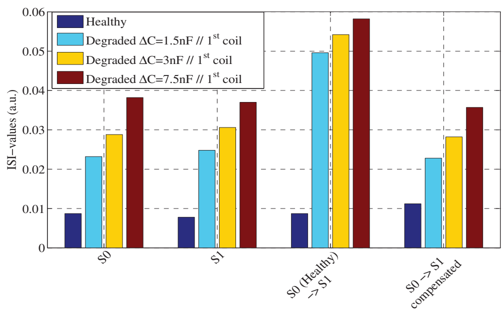

Fig. 6 Insulation state indicators for different machine states analyzed with different sensors and in case of a sensor exchange.

B. *Investigations of currrent sensor operating point*

In this section investigations of the operating point of the sensor are analyzed. While at current transducers based on open loop, at which the current induces a magnetic field in the core whose magnetic flux density is sensed in the air gap by the Hall-sensor and delivers an output voltage, the Hall generator voltage at closed loop is used to create a compensation current in the secondary coil around the core that compensates the flux in the iron core to zero. At zero flux the magnetic potential, also referred as ampere-turns in the two conductors are equal and the secondary current is the transformed primary current $I_S = I_P N_P / N_S$, with the ratio N_P / N_S the number of turns. Due to the compensation of the flux, the linear region of the hysteresis loop regarding the iron magnetization has not to be considered at closed loop sensors.

However, influences at which the behavior of the sensor at a specific operating point is affected still exist. The closed loop sensors reacts instantaneously to a current level with a small reaction delay typically far below $1\mu s$. So, in addition to DC and AC currents also impulse currents can be accurately measured. With the additional internal components, e.g. the compensation coil, operational amplifier, power amplifiers, bypass diodes etc., the fast response of the feedback system is determined. In addition to a possible drift of the operational amplifier and the Hall sensor due to temperature variations, it may also lead to a non-linear behavior at the zero crossing depending on how the output stage is constructed in the sensor. In the aforementioned sections the operating point of the current sensor is disregarded and the measurements were conducted at stand still without magnetization of the machine. The sensor is working at its zero crossing and measures zero current before the voltage step is applied to the machine. To analyze the influence of the sensor operating point, a bias current of 20A is induced into the machine by a simple PI controller, as can be seen in Fig. 7 (a) and (b).

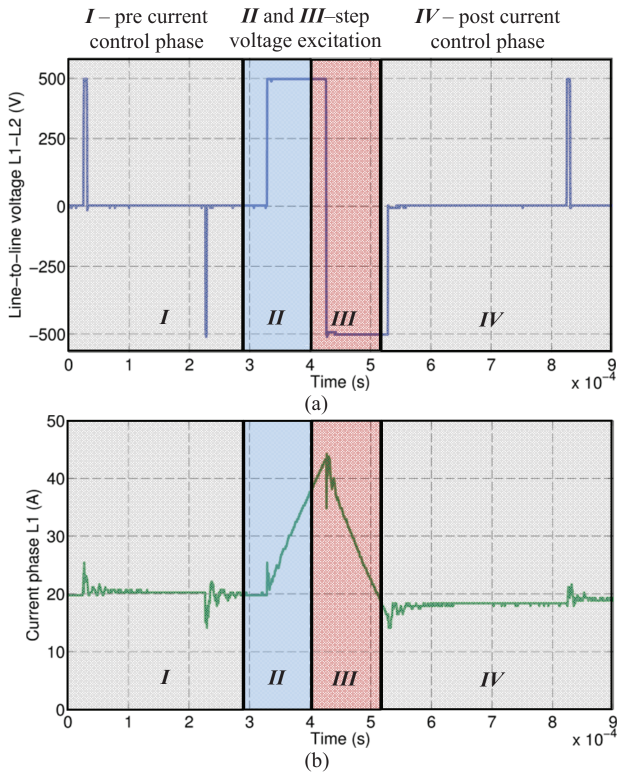

Fig. 7 (a) Line-to-line voltage L1-L2 sequence of the current control and measurement procedure. (b) corresponding current response of phase L1.

In the upper subfigure (a) a short sequence of the line-to-line voltage L1-L2 during the control and measurement process is shown, starting with a short positive pulse, followed by the equivalent negative switching transition with shorter duration to ensure the positive current injection (***I***). Afterwards the test excitation pulse to excite the machine's transient current reaction is visible for about $200\mu s$ (***II*** and ***III***). Finally, the current control adjusts the selected current value in several PWM-cycles to enable the repetition of the measurement (***IV***). The pulse width for the transient measurement in ***I*** and ***II*** respectively is set to $100\mu s$ to ensure that the current slope is accurately recorded and the oscillation is decayed. In further tests the duration was set to a minimum of $30\mu s$, which is the actual limit in order to record the transient and accurately calculate the mean current slope.
The same signal processing as described in chapter II is applied. Again, this is done for different machine scenarios at which the insulation degradation is emulated by different capacitors in parallel to the winding. That means at different bias currents and machine insulation state scenarios the transient current response are investigated. The results are depicted in Fig. 8. On the x-axis of the bar plot, the machine insulation state scenarios at different induced bias currents are depicted. The value of the induced current is specified in percentage of the nominal current of I_N=1000A of the sensor. Due to the injected current a significant rise of the indicators are observable. Compared to the measurement at which zero crossing of the sensor occurs or is located within this oscillation range, the sensitivity of the process can be improved.

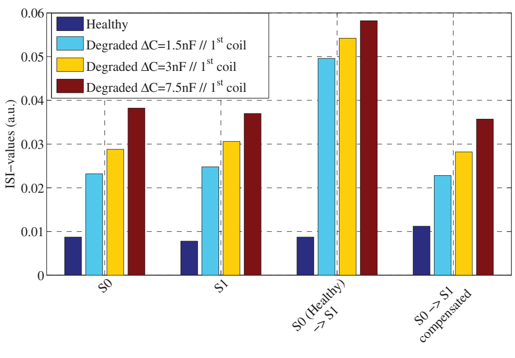

Fig. 8 Insulation state indicators for different machine states analyzed at different operating points of the same current sensor.

In Fig. 9 the current trace is starting at 'I_{L1}=-20A' and with a positive switching state in the corresponding phase the current is driven into the positive region to up to 'I_{L1}=-20A'. Two main effects can be observed due to the signal trace. At zero-crossing and passing the horizontal line of '0A' the commutation of the inverter free-wheeling diode, driving the negative current, to the transistor can be seen. This is depicted in the enlarged subfigure *I*. After zero-crossing, an undefined state in the internal power amplifier of the current sensor shows a step in the current slope with a high variance (±σ), as can be seen in subfigure *II*. It is suspected that the trace is not accurately reproduced by the typically used complementary transistor amplifier of the sensor electronic (NPN and PNP) as the transition occurs, when they are switching over from one transistor to the other. Both transistors have a 0.7V area in which they are not conducting and the current is flowing over a bypassed freewheeling circuit. This so-called crossover distortion produces a non-linear output wave shape. If the sensor hardware is not implemented with crossover distortion compensation, the insulation monitoring method has to be enhanced with focus on the correct operation point influence of the sensor.

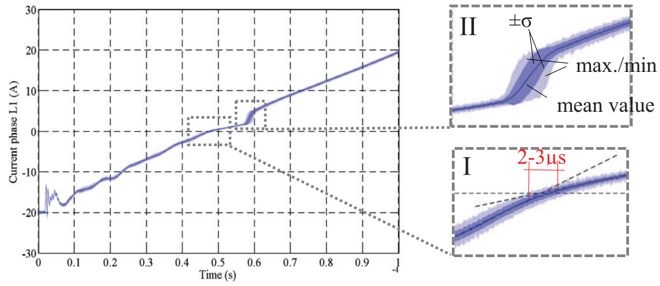

Fig. 9 Current trace of phase L1 during zero-crossing of the sensor.

The non-linear behavior can also be observed if the input output signals are analyzed with sinusoidal signals of different frequency. Fig. 10 shows the Lissajous-graph of the input-output signals of the sensors at a selected frequency of 400kHz, which is in the interesting frequency range for the insulation state estimation. On the y-axis the magnitude of the primary conductor signal through the sensor and on the x-axis the output magnitude of the sensor with the transformed ratio *N1/N2* is depicted. In the left subfigure (a) the Lissajous-graph show a phase shift of the two signals. By injection of a DC bias-current the graph changes the shape to a straight line, indicating that no phase shift between input and output signal exist. The input current is accurately reproduced with transmission ratio.

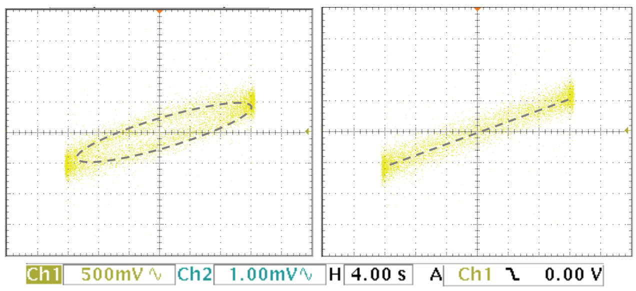

(a) (b)

Fig. 10 Lissajous-graph of primary current through the current transducer (CH1) and output current of transducer (CH2).

III. Conclusion

A method to detect insulation degradation by transient current signal evaluation after step excitation with the inverter is presented. The usage of the built-in current transducers is one of the key targets to safe space and costs for the system. A compensation strategy to prevent influences through the variance between sensors of the same production batch was shown. Due to this approach a sensor hardware exchange is possible using a compensation function. Additionally, influences through the operating point of the sensor were analyzed and methods are presented to avoid the influence of non-linearity.

Acknowledgment

The work to this investigation was supported by the Austrian Research Promotion Agency (FFG) under project number 838478.

References

[1] Zoeller, C.; Winter, T.; Wolbank, T.M.; Vogelsberger, M.A.; Bazant, M., “Separation of fundamental wave and transient components of the current signal for machine insulation state monitoring,” *40th Annual Conference of the IEEE Industrial Electronics Society, IECON*, pp.4498-4504, 2014.

[2] Nussbaumer, P.; Vogelsberger, M.A.; Wolbank, T.M., “Exploitation of induction machine's high-frequency behavior for online insulation monitoring,” *9th IEEE International Symposium on Diagnostics for Electric Machines, Power Electronics and Drives (SDEMPED)*, pp.579-585, 2013.

[3] Persson, E., “Transient effects in application of PWM inverters to induction motors,” *IEEE Transactions on Industry Applications*, vol.28, no.5, pp.1095-1101, 1992.

[4] Nussbaumer, P.; Zoeller, C.; Wolbank, T.M.; Vogelsberger, M.A., “Transient distribution of voltages in induction machine stator windings resulting from switching of power electronics,” *39th Annual Conference of the IEEE Industrial Electronics Society, IECON*, pp.3189-3194, 2013.

[5] Stone, G. C.; Boulter, E. E.; Culbert, I.; Dhirani, H., “Electrical Insluation for Rotating Machines”. *IEEE Press*, 2004.

[6] Toliyat, Hamid A., et al. “Electric Machines: Modeling, Condition Monitoring, and Fault Diagnosis”. *CRC Press*, 2012.

[7] Zhang, P. ; Du, Y.; Habetler, T. G. ; Lu, B., “A survey of condition monitoring and protection methods for medium-voltage induction motors,” IEEE Trans. Ind. Appl., vol. 47, no. 1, pp. 34–46, 2011.

[8] IEEE Committee Report; “Report of large motor reliability survey of industrial and commercial installation, Part I,” *IEEE Transactions on Industry Applications*, vol.21, no.4, pp.853–864, 1985.

[9] IEEE Committee Report; “Report of large motor reliability survey of industrial and commercial installation, Part II,” *IEEE Transactions on Industry Applications,* vol.21, no.4, pp.865–872, 1985.

[10] Zoeller, C.; Vogelsberger, M.A.; Fasching, R.; Grubelnik, W.; Wolbank, Th.M., “Evaluation and current-response based identification of insulation degradation for high utilized electrical machines in railway application,” 2015 IEEE 10th International Symposium on Diagnostics for Electrical Machines, Power Electronics and Drives (SDEMPED), pp.266-272, 2015.

[11] Farahani, M.; Gockenbach, E.; Borsi, H.; Schäfer, K.; Kaufhold, M.; “Behavior of machine insulation systems subjected to accelerated thermal aging test,” *IEEE Transactions on Dielectrics and Electrical Insulation*, vol.17, no.5, pp.1364-1372, 2010.

[12] Perisse, F.; Werynski, P.; Roger, D., "A New Method for AC Machine Turn Insulation Diagnostic Based on High Frequency Resonances," *Dielectrics and Electrical Insulation, IEEE Transactions on* , vol.14, no.5, pp.1308,1315, October 2007.

[13] Peroutka, Z.; Kus, V., “Adverse effects in voltage source inverter-fed drive systems,” *17th Annual IEEE Conference and Exposition on Applied Power Electronics, APEC*, vol.1, pp.557-563, 2002.